



<https://doi.org/10.15407/ufm.26.01.003>

V.A. TATARENKO*, **T.M. RADCHENKO****,
A.Yu. NAUMUK***, and **B.M. MORDYUK******

G.V. Kurdyumov Institute for Metal Physics of the N.A.S. of Ukraine,
36 Academician Vernadsky Blvd.,
UA-03142 Kyiv, Ukraine

* tatar@imp.kiev.ua, ** tarad@imp.kiev.ua,
*** artem.naumuk@gmail.com, **** mordyuk@imp.kiev.ua

PARAMETERIZATION OF DIFFUSION CHARACTERISTICS OF ATOMIC-ORDER RELAXATION KINETICS IN Ni–Al ALLOYS

To study diffusion characteristics in substitutional f.c.c.-Ni–Al alloys, we review, analyse, and use the kinetic models, in which the relaxation of correlation parameters for the atomic distribution causes the time dependence of both the diffuse-scattering intensity I and the residual electrical resistivity ρ . Using the parameterization of the available literature data about the measurement of the residual electrical resistivity during the isothermal annealing of alloys, the most characteristic relaxation times of ρ after quenching of the alloys and its equilibrium value ρ_{∞} are estimated. The maximum characteristic relaxation time of the atomic order of such alloys is determined, and the curves of the time dependence of the normalized change in intensity ΔI are predicted based on the hypothesis of the coincidence of the largest characteristic relaxation times for I and ρ . The relaxation process is accompanied by both the increase in the number of clusters with the presence of short-range order in their structure and the degree of their order that is consistent with both the results of computer modelling of local atomic ordering using the Monte Carlo method and the model of inhomogeneous short-range order.

Keywords: Ni–Al solid solution, atomic jumps, diffusion, short-range order, relaxation, diffuse scattering, residual resistivity.

Citation: V.A. Tatarenko, T.M. Radchenko, A.Yu. Naumuk, and B.M. Mordyuk, Parameterization of Diffusion Characteristics of Atomic-Order Relaxation Kinetics in Ni–Al Alloys, *Progress in Physics of Metals*, **26**, No. 1: 3–25 (2025)

© Publisher PH “Akademperiodyka” of the NAS of Ukraine, 2025. This is an open access article under the CC BY-ND license (<https://creativecommons.org/licenses/by-nd/4.0>)

1. Introduction

Short-range order (SRO) in a single-phase solid solution represents concentration inhomogeneities, the linear scales of which are comparable to the average interatomic distances. Since each temperature corresponds to its equilibrium SRO, a rapid hardening from one (disordered) state to another should lead to the relaxation of the initial degree of SRO to its new (equilibrium) value. This relaxation kinetic process is carried out due to the diffusion of atoms at a distance of the order of average interatomic magnitude, since the SRO for distant co-ordination spheres is, as a rule, almost zero.

A.G. Khachaturyan [1, 2] proposed a theory for diffusional relaxation of SRO in a multicomponent substitutional solid solution. As shown, the time dependences of SRO parameters and the intensity of diffuse scattering (of x-rays or thermal neutrons) associated (caused) with (by) SRO can be used to study elementary acts of diffusion, *i.e.*, to determine the probabilities of atomic jumps per unit of time to different lattice sites and to obtain ‘macroscopic’ diffusion characteristics, namely, activation energies and (self)diffusion coefficients for atoms. The method proposed in Refs. [1, 2] is currently the only one possible for studying (using diffraction experimental data) the elementary diffusion acts in the case of ‘slow’ diffusion. (Elementary acts in the case of ‘fast’ diffusion, when the duration of the settled life of the atom of the diffusing component is less than the lifetime of the excited state of the nucleus of this component, can be studied according to the broadening of Mößbauer lines of resonant absorption of γ -ray quanta [3].) Note that, in all traditional methods for studying the diffusion, the linear dimensions of concentration inhomogeneities far exceed the crystal-lattice parameters; the diffusion parameters obtained with the application of these methods are, actually, the coefficients of the continuum equations of macroscopic diffusion and do not contain direct information about the elementary acts and mechanisms of atomic diffusion.

For a binary alloy with small deviations of non-equilibrium structural characteristics from their equilibrium values, the time dependence of the intensity of elastic diffuse scattering of rays for the point \mathbf{k} of the reciprocal space, which is caused by the diffusional relaxation of SRO and, first of all, the migration of atoms of the slowest component (*e.g.*, the first one), is evaluated as [1, 2]

$$\Delta I(\mathbf{k}, t) \equiv I(\mathbf{k}, t) - I(\mathbf{k}, \infty) \cong [I(\mathbf{k}, 0) - I(\mathbf{k}, \infty)] e^{-2\lambda_1(\mathbf{k})t};$$

here, $I(\mathbf{k}, \infty)$ is a diffuse scattering intensity of the ‘equilibrium’ solid solution, which corresponds to the annealing time $t \rightarrow \infty$; $I(\mathbf{k}, 0)$ is the intensity that corresponds to the initial instant of annealing time $t = 0$ (the state of only just hardened alloy); $2\lambda_1(\mathbf{k})$ is the reciprocal value of relaxation time of the intensity corresponding to the given wave vector \mathbf{k} . The

latter equation is valid [4, 5] only when

$$\frac{\lambda_1(\mathbf{k})}{\lambda_2(\mathbf{k})} \cong \frac{e^{-Q_1/(k_B T)}}{e^{-Q_2/(k_B T)}} \ll 1 \text{ and } \lambda_1(\mathbf{k})t_0 \cong 1,$$

where $2\lambda_2(\mathbf{k})$ is the reciprocal relaxation time of intensity attributed to the diffusion of atoms of a faster component (e.g., the second one), Q_1 and Q_2 are the activation energies of atomic diffusion of the first and second components, respectively, and t_0 is a characteristic time of the observed intensity change. According to the kinetic formula for $\Delta I(\mathbf{k}, t)$, the time evolution of the diffuse-scattering intensity $I(\mathbf{k}, t)$ is described by one relaxation time and is carried out due to the diffusion of atoms of the ‘slow’ component (atoms of the ‘faster’ component adiabatically adjust to the movement of the slow component). In addition, we assume that the relaxation of the intensity $I(\mathbf{k}, t)$ for each point of the reciprocal space occurs independently of the others with its own relaxation time.

The $\lambda_1(\mathbf{k})$ and $\lambda_2(\mathbf{k})$ values can be written [4, 5] as

$$\lambda_1(\mathbf{k}) = \lambda_1^0(\mathbf{k})[1 + \varphi_1(\mathbf{k})] \text{ and } \lambda_2(\mathbf{k}) = \lambda_2^0(\mathbf{k})[1 + \varphi_2(\mathbf{k})],$$

where $\lambda_1^0(\mathbf{k})$ and $\lambda_2^0(\mathbf{k})$ relate to the reciprocal times of the diffusion relaxation of atoms of the first and second components in the perfect solid solution. The $\varphi_1(\mathbf{k})$ and $\varphi_2(\mathbf{k})$ functions describe the influence of the imperfection of solid solution on the atomic diffusion (in the perfect solution, $\varphi_1(\mathbf{k}) = \varphi_2(\mathbf{k}) \equiv 0$). The $-\lambda_\alpha^0(\mathbf{k})$ value is defined by the Fourier transform of the probabilities of elementary jumps of α -type atoms from all (‘zero’) sites of the surroundings into the certain \mathbf{r} site per unit of time in the perfect solution, $-\lambda_\alpha(\mathbf{k})$ is an analogous value for the imperfect solution, and the Fourier original $-\Lambda_\alpha(\mathbf{r})$ is the probability of an elementary jump of α -atom per unit of time to the \mathbf{r} site from any neighbouring ‘zero’ site, which occurs in the ‘potential’ field generated by the concentration inhomogeneity of α -type atoms in the ‘zero’ site ($\alpha = 1, 2$). According to Ref. [2], the continuous analogue of the above expressions for $\lambda_\alpha(\mathbf{k})$ ($\lambda_1(\mathbf{k})$ and $\lambda_2(\mathbf{k})$) is the Darken equation [6]:

$$D_\alpha \approx D_\alpha^0 \left(1 + \frac{d \ln \gamma_\alpha}{d \ln c_\alpha} \right),$$

with D_α , D_α^0 , and γ_α being the coefficients of diffusion, self-diffusion, and the activity coefficient of the α -component, respectively. At a continuum approximation of small $|\mathbf{k}| = k \ll 2\pi/a$ [4, 5],

$$\lambda_\alpha(\mathbf{k}) \cong D_\alpha k^2, \quad \lambda_\alpha^0(\mathbf{k}) \cong D_\alpha^0 k^2, \quad \varphi_\alpha(\mathbf{k}) \cong \frac{d \ln \gamma_\alpha}{d \ln c_\alpha},$$

at least, for a cubic solution.

Thus, the main relations of Khachaturian’s theory [1, 2] make it possible to use the data of the method of diffuse scattering of x-rays by single

crystals of disordered solutions for the direct determination of the characteristics of the elementary diffusion acts: the Fourier components of the probabilities of atomic jumps, $-\lambda_\alpha(\mathbf{k})$, and the values of the probabilities in the real space, $-\Lambda_\alpha(\mathbf{r})$. Using equations of the latter type, it is possible to determine the coefficients and activation energies of (self)diffusion. Knowing the $-\Lambda_\alpha(\mathbf{r})$, we can establish the diffusion mechanism of the elementary acts of diffusion: ring, vacancy, or interstitial.

Within the framework of such an approach, the structure formation of the Ni-based alloys (*e.g.*, Ni–Mo, Ni–Fe, *etc.*) was studied in the series of works (see, *e.g.*, Refs. [7–50]). In this work, we initially review and analyse the literature data on such diffusion processes in f.c.c.-Ni–Al alloy, and then, parameterise its diffusion characteristics during the atomic-order relaxation taking into account its specific features.

2. Scheme to Estimate the Probabilities of Atomic Jumps

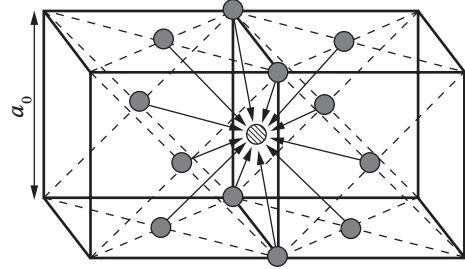
As mentioned in the Introduction, data on the kinetics of diffuse scattering associated with the SRO make it possible to determine the characteristics of elementary acts of diffusion, namely, the probabilities of jumps of atoms of different types to different lattice sites. Each temperature and concentration of the alloy correspond to its equilibrium degree (parameter) of SRO. A rapid quenching from a high-temperature disordered state to another, low-temperature state should lead to relaxation of the initial degree of SRO to its new equilibrium value. Since this relaxation is realised due to the (interstitial) migration of atoms at the intersite distances, studying this process opens up possibilities for examining the elementary acts of diffusion.

As mentioned above, from the values of $\lambda_\alpha(\mathbf{k})$, we can calculate the Fourier originals $\{-\Lambda_\alpha(\mathbf{R})\}$, which have a sense of the probabilities of α -atoms' jumps per unit of time on the site \mathbf{R} from all surrounding sites $\{\mathbf{R}'\}$ in the field of 'interaction potential' $\psi_\alpha(\mathbf{R}')$. Assume that 'potential' $\psi_\alpha(\mathbf{R}')$ is generated, if the microscopic concentration inhomogeneity occurs, *e.g.*, through the localization of α -atom at the 'zero' ('central') site. So, $\psi_\alpha(\mathbf{R}')$ represents the effect of the 'potential' field due to concentration inhomogeneities (of the SRO-type) in an imperfect alloy. The alloy is perfect, if there is no such effect. $\Lambda_\alpha(\mathbf{R})$ for each \mathbf{R} (including a 'zero' site) in the crystal lattice is proportional to all $\{\psi_\alpha(\mathbf{R}')\}$ values. Using the inverse Fourier transform in the \mathbf{R} -space, we can express $\Lambda_\alpha(\mathbf{R})$ as [4, 5]

$$\Lambda_\alpha(\mathbf{R}) \cong \frac{c(1-c)}{k_B T} \sum_{\mathbf{R}'} \Lambda_\alpha^0(\mathbf{R} - \mathbf{R}') \psi_\alpha(\mathbf{R}'),$$

where $-\Lambda_\alpha^0(\mathbf{R} - \mathbf{R}')$ represents a probability of a jump of α -type atom (per unit of time) from any \mathbf{R}' site into the \mathbf{R} site in a perfect solid solution,

Fig. 1. Atomic jumps into the given site (striped circle) from the nearest sites (grey circles) in f.c.c. lattice [51]



for which $\{\psi_\alpha(\mathbf{R}')\}$ ‘potentials’ are equal to ψ_0 , c is a relative atomic fraction of α -atoms. The values of $\Lambda_\alpha(\mathbf{R})$ depend on the mutual location of the lattice sites for this syngony, that is, on the set of possible differences $\{\mathbf{R} - \mathbf{R}'\}$ for each \mathbf{R} . In the case of the classical vacancy mechanism of diffusion, commonly, the atomic jumps only at the distance between the nearest sites are taken into account (Fig. 1) [51]. When it is necessary to check the possibility of another diffusion mechanism, we should consider several sets of values: $\{\Lambda_\alpha^0(\mathbf{R} - \mathbf{R}'_I)\}$, $\{\Lambda_\alpha^0(\mathbf{R} - \mathbf{R}'_{II})\}$, *etc.* Indices I, II, *etc.* refer to jumps to the \mathbf{R} site from the nearest neighbouring sites $\{\mathbf{R}'_I\}$, next neighbouring sites $\{\mathbf{R}'_{II}\}$, *etc.*

Let us assume that $\psi_\alpha(\mathbf{R}')$ is a non-zero function within the first six co-ordination shells around the ‘zero’ site only, while the atomic-jump probability has non-zero values for two co-ordination shells only [52],

$$\Lambda_\alpha^0(\mathbf{0}) = \Lambda_{\alpha 0}^0 \neq 0, \quad \Lambda_\alpha^0(R_I) = \Lambda_{\alpha I}^0 \neq 0, \quad \Lambda_\alpha(R_{II}) = \Lambda_{\alpha II}^0 \neq 0,$$

$$\psi_\alpha(\mathbf{0}) = \psi_{\alpha 0} \neq 0, \quad \psi_\alpha(R_I) = \psi_{\alpha I} \neq 0, \quad \psi_\alpha(R_{II}) = \psi_{\alpha II} \neq 0, \quad \psi_\alpha(R_{III}) = \psi_{\alpha III} \neq 0$$

$$\psi_\alpha(R_{IV}) = \psi_{\alpha IV} \neq 0, \quad \psi_\alpha(R_V) = \psi_{\alpha V} \neq 0, \quad \psi_\alpha(R_{VI}) = \psi_{\alpha VI} \neq 0,$$

where R_I, R_{II}, \dots are the radii of the first, second, ... co-ordination shells, whereas other probabilities $\Lambda_{\alpha III}^0, \Lambda_{\alpha IV}^0, \dots$ and values of $\psi_{\alpha VII}, \psi_{\alpha VIII}, \dots$ are equal to zero. For certainty, let us assume that α -atom is localized at the ‘0’-site (with $\mathbf{R} = \mathbf{0}$). Then, we have [52]:

$$\Lambda_\alpha(\mathbf{R}_0(000)) \cong 12\Lambda_{\alpha I}^0 \left(\frac{\psi_{\alpha I}}{\psi_0} \right) + 6\Lambda_{\alpha II}^0 \left(\frac{\psi_{\alpha II}}{\psi_0} \right) + \Lambda_{\alpha 0}^0 \left(\frac{\psi_{\alpha 0}}{\psi_0} \right),$$

$$\Lambda_\alpha(\mathbf{R}_I(110)) \cong 4\Lambda_{\alpha I}^0 \left(\frac{\psi_{\alpha I}}{\psi_0} \right) + 2\Lambda_{\alpha II}^0 \left(\frac{\psi_{\alpha II}}{\psi_0} \right) + \Lambda_{\alpha I}^0 \left(\frac{\psi_{\alpha III}}{\psi_0} \right) +$$

$$+ 4\Lambda_{\alpha I}^0 \left(\frac{\psi_{\alpha IV}}{\psi_0} \right) + 2\Lambda_{\alpha II}^0 \left(\frac{\psi_{\alpha I}}{\psi_0} \right) + \Lambda_{\alpha 0}^0 \left(\frac{\psi_{\alpha I}}{\psi_0} \right) + \Lambda_{\alpha I}^0 \left(\frac{\psi_{\alpha 0}}{\psi_0} \right),$$

$$\Lambda_\alpha(\mathbf{R}_{II}(200)) \cong 4\Lambda_{\alpha I}^0 \left(\frac{\psi_{\alpha I}}{\psi_0} \right) + 4\Lambda_{\alpha I}^0 \left(\frac{\psi_{\alpha IV}}{\psi_0} \right) + \Lambda_{\alpha II}^0 \left(\frac{\psi_{\alpha VI}}{\psi_0} \right) +$$

$$\begin{aligned}
 & +4\Lambda_{\alpha\text{II}}^0 \left(\frac{\Psi_{\alpha\text{III}}}{\Psi_0} \right) + \Lambda_{\alpha 0}^0 \left(\frac{\Psi_{\alpha\text{II}}}{\Psi_0} \right) + \Lambda_{\alpha\text{II}}^0 \left(\frac{\Psi_{\alpha 0}}{\Psi_0} \right), \\
 \Lambda_{\alpha}(\mathbf{R}_{\text{III}}(211)) & \cong 2\Lambda_{\alpha\text{I}}^0 \left(\frac{\Psi_{\alpha\text{I}}}{\Psi_0} \right) + \Lambda_{\alpha\text{I}}^0 \left(\frac{\Psi_{\alpha\text{II}}}{\Psi_0} \right) + 2\Lambda_{\alpha\text{I}}^0 \left(\frac{\Psi_{\alpha\text{III}}}{\Psi_0} \right) + 2\Lambda_{\alpha\text{I}}^0 \left(\frac{\Psi_{\alpha\text{IV}}}{\Psi_0} \right) + \\
 \Lambda_{\alpha}(\mathbf{R}_{\text{IV}}(220)) & \cong \Lambda_{\alpha\text{I}}^0 \left(\frac{\Psi_{\alpha\text{I}}}{\Psi_0} \right) + 4\Lambda_{\alpha\text{I}}^0 \left(\frac{\Psi_{\alpha\text{IV}}}{\Psi_0} \right) + \\
 & + 2\Lambda_{\alpha\text{II}}^0 \left(\frac{\Psi_{\alpha\text{II}}}{\Psi_0} \right) + 2\Lambda_{\alpha\text{II}}^0 \left(\frac{\Psi_{\alpha\text{V}}}{\Psi_0} \right) + \Lambda_{\alpha 0}^0 \left(\frac{\Psi_{\alpha\text{III}}}{\Psi_0} \right), \\
 \Lambda_{\alpha}(\mathbf{R}_{\text{V}}(310)) & \cong \Lambda_{\alpha\text{I}}^0 \left(\frac{\Psi_{\alpha\text{II}}}{\Psi_0} \right) + \Lambda_{\alpha\text{I}}^0 \left(\frac{\Psi_{\alpha\text{III}}}{\Psi_0} \right) + \\
 & + \Lambda_{\alpha\text{I}}^0 \left(\frac{\Psi_{\alpha\text{IV}}}{\Psi_0} \right) + \Lambda_{\alpha\text{I}}^0 \left(\frac{\Psi_{\alpha\text{VI}}}{\Psi_0} \right) + \Lambda_{\alpha\text{II}}^0 \left(\frac{\Psi_{\alpha\text{I}}}{\Psi_0} \right), \\
 \Lambda_{\alpha}(\mathbf{R}_{\text{VI}}(222)) & \cong 3\Lambda_{\alpha\text{I}}^0 \left(\frac{\Psi_{\alpha\text{IV}}}{\Psi_0} \right) + 3\Lambda_{\alpha\text{II}}^0 \left(\frac{\Psi_{\alpha\text{III}}}{\Psi_0} \right) + \Lambda_{\alpha 0}^0 \left(\frac{\Psi_{\alpha\text{V}}}{\Psi_0} \right), \\
 \Lambda_{\alpha}(\mathbf{R}_{\text{VII}}(321)) & \cong \Lambda_{\alpha\text{I}}^0 \left(\frac{\Psi_{\alpha\text{III}}}{\Psi_0} \right) + \Lambda_{\alpha\text{I}}^0 \left(\frac{\Psi_{\alpha\text{IV}}}{\Psi_0} \right) + \Lambda_{\alpha\text{I}}^0 \left(\frac{\Psi_{\alpha\text{V}}}{\Psi_0} \right) + \Lambda_{\alpha\text{II}}^0 \left(\frac{\Psi_{\alpha\text{IV}}}{\Psi_0} \right), \\
 \Lambda_{\alpha}(\mathbf{R}_{\text{VIII}}(400)) & \cong 4\Lambda_{\alpha\text{I}}^0 \left(\frac{\Psi_{\alpha\text{VI}}}{\Psi_0} \right) + \Lambda_{\alpha\text{II}}^0 \left(\frac{\Psi_{\alpha\text{II}}}{\Psi_0} \right).
 \end{aligned}$$

Here, (lmn) for $\Lambda_{\alpha}(\mathbf{R}_n(lmn))$ are the co-ordinates of sites in a cubic lattice with translation vectors $[100]$, $[010]$, and $[001]$ along the Ox , Oy , and Oz axis directions, respectively (we mean the co-ordinates (lmn) in the units of $a_0/2$, where a_0 is an f.c.c.-lattice parameter). The $-\Lambda_{\alpha 0}^0$ is a probability (per unit of time) for α -atom to remain in the fixed site; $\Psi_{\alpha 0}$ is a value of the ‘potential’ function at the ‘zero’ site. The value of $\Lambda_{\alpha}(\mathbf{R}_n(lmn))$ can be calculated from the inverse Fourier transform of the $\lambda_{\alpha}(\mathbf{k})$ values, which can be estimated, based on the kinetic model using the available experimental data for Ni–Al. The Fourier original of the atomic-jump probability to the site \mathbf{R} of the f.c.c. lattice is as follows:

$$\Lambda_{\alpha}(\mathbf{R}) = K(lmn) \sum_{k_1 k_2 k_3} \lambda_{\alpha}(k_1 k_2 k_3) \cos(2\pi k_1 l) \cos(2\pi k_2 m) \cos(2\pi k_3 n),$$

where K is a ‘geometric’ coefficient dependent on $\mathbf{R}(lmn)$. Macroscopic diffusion characteristics, *i.e.*, diffusion and self-diffusion coefficients of ‘slow’ α -ions can be calculated from the probabilities of atomic jumps. Using the long-wavelength limit transition from a discrete migration process

to a continuous transfer along with the assumption of equally probable atomic jumps to sites within the same co-ordination shell (relative to the 'zero' site), we can write for diffusion mobilities in perfect (D_α^*) and imperfect (D_α) cubic solutions [53]:

$$D_\alpha^* \approx -\frac{1}{6} \sum_{n=1}^{\infty} \Lambda_\alpha^0(R_n) R_n^2 Z_n, \quad D_\alpha \approx -\frac{1}{6} \sum_{n=1}^{\infty} \Lambda_\alpha(R_n) R_n^2 Z_n$$

(Z_n is a co-ordination number of the n -th co-ordination shell of the R_n radius). The latter expressions establish a relationship between the $\lambda_{Ni}(\mathbf{k})$ and $\lambda_{Ni}^0(\mathbf{k})$ values and the diffusion and self-diffusion coefficients. Indeed, the values of $\lambda_{Ni}(\mathbf{k})$ for imperfect solid solution relate to the probabilities of intersite jumps $-\Lambda_{Ni}(\mathbf{r})$:

$$\lambda_{Ni}(\mathbf{k}) = \sum_{n=1}^{\infty} \sum_{\mathbf{r}_n} -\Lambda_{Ni}(\mathbf{r}_n) (1 - e^{-i\mathbf{k} \cdot \mathbf{r}_n}),$$

where $|\mathbf{r}_n| = r_n (> 0)$ is the radius of the n -th co-ordination shell. To obtain the latter expression, the Ni-atoms' number constancy condition $\lambda_{Ni}(\mathbf{k} = \mathbf{0}) \equiv 0$ [4] is used. Expansion of $e^{-i\mathbf{k} \cdot \mathbf{r}_n}$ into a series and restrictions in the case of small \mathbf{k} by the first three terms give:

$$\lambda_{Ni}(\mathbf{k}) \cong -\frac{k^2}{6} \sum_{n=1}^{\infty} \Lambda_{Ni}(\mathbf{r}_n) r_n^2 Z_n.$$

Comparing the latter equation with above-mentioned continuum approximation, we have an expression for diffusivity D_{Ni} :

$$D_{Ni} \cong -\frac{1}{6} \sum_n \Lambda_{Ni}(r_n) r_n^2 Z_n.$$

For a perfect solid solution (in the commonly used approximation of Ni-atoms' jumps on the nearest distance r_1 only), the formulas for $\lambda_{Ni}^0(\mathbf{k})$ and self-diffusion coefficient D_{Ni}^* are, respectively,

$$\lambda_{Ni}^0(\mathbf{k}) = -\Lambda_{Ni}^0(r_1) \sum_{\mathbf{r}_1} (1 - e^{-i\mathbf{k} \cdot \mathbf{r}_1}), \quad D_{Ni}^* = -\frac{1}{6} \Lambda_{Ni}^0(r_1) r_1^2 Z_1.$$

3. Kinetic Parameters of Atomic Migration and Scattering Relaxation of Different-Types' Waves

The Ni–Al binary alloy, at least, in a narrow concentration range close to the Ni₃Al composition, can be ordered as the $L1_2$ -type [54] based on the f.c.c. lattice up to the melting temperature ($\cong 1636$ – 1658 K) [55]. The study of the kinetics of the ordering of such a (non-)stoichiometric crystalline compound is of interest for solving the problem of the stability of its structure under conditions of high-temperature heating, since the $L1_2$ -Ni₃Al-type phases are the base of modern heat-resistant materials, and the coatings based on them have a high catalytic activity.

Both direct and indirect methods can be used to study the kinetics of SRO relaxation in substitutional alloys [4, 53]. Direct (diffraction) meth-

ods include the use of data on the time dependence of diffuse scattering of radiations. An example of an indirect method is the use of data on the time evolution of physical properties due to the SRO; the measurement of residual electrical resistivity is the most often used in this aspect.

Let us introduce the two-particle correlation function $P_{\alpha\beta}(\mathbf{r}, t)$ as the probability that α - and β -atoms ($\alpha, \beta = \text{Ni, Al}$) are located simultaneously (in the instant of time t) on the distant \mathbf{r} from each other (with \mathbf{r} acting as a difference of appropriate radius-vectors of the Bravais lattice). Then, for a binary Ni–Al substitutional alloy, one can show [5] that the time dependence of its Fourier components behaves in a relaxed manner.

In all realistic cases of binary substitutional solutions, the inequality

$$\frac{\lambda_1(\mathbf{k})}{\lambda_2(\mathbf{k})} \propto \frac{e^{-E_{a1}/(k_B T)}}{e^{-E_{a2}/(k_B T)}} \ll 1$$

turns out to be valid as a result of any noticeable difference in the thermal activation energies E_{a1} and E_{a2} of relaxation processes according to the first and second ‘scenarios’, respectively; this inequality is fulfilled, if the diffusion coefficients of both components differ significantly. Taking into account this circumstance and substituting, we can get as follow:

$$\frac{\Delta I(\mathbf{k}, t)}{\Delta I(\mathbf{k}, 0)} \cong e^{-2\lambda_1(\mathbf{k})t}$$

that corresponds to the so-called 1st-order kinetic model, when $\lambda_1(\mathbf{k}) \ll \ll \lambda_2(\mathbf{k})$, or

$$\frac{\Delta I(\mathbf{k}, t)}{\Delta I(\mathbf{k}, 0)} \approx A_1 e^{-2\lambda_1(\mathbf{k})t} + A_2 e^{-\lambda_2(\mathbf{k})t}$$

for a more realistic 2nd-order kinetics model, when non-equality $\lambda_1(\mathbf{k}) < \lambda_2(\mathbf{k})$ is more ‘soft’, with A_1 and A_2 being the ‘weights’ of the first and second ‘scenarios’, respectively. Then, for the intensity-relaxation times, the following approximate expressions are valid: $\tau \cong 1/[2\lambda_1(\mathbf{k})]$ within the 1st-order kinetics model and $\tau_1 \approx 1/[2\lambda_1(\mathbf{k})]$, $\tau_2 \approx 1/\lambda_2(\mathbf{k})$ for the 2nd-order kinetics model. Thus, in the first (second) kinetics model, the time evolution of the intensity of the diffuse scattering of radiations (and of SRO) is characterized by one (two) relaxation time(s).

To study the SRO kinetics relaxation by the resistometric method (*i.e.*, based on the time dependence of the specific residual electrical resistance during isothermal annealing of a solid solution), we assume that the rates of change of the SRO degree and, accordingly, the electrical resistivity are proportional to the appropriate ‘thermodynamic forces’ as functions F of the deviation from equilibrium. Then, the ‘general’ equation of the kinetics of the process can be written as, for instance,

$$\frac{\partial \rho(t, T_a)}{\partial t} \approx -F(\{\tau_i^{-1}\}; \rho(t, T_a) - \rho_\infty(T_a)),$$

where $\rho(t, T_a)$ and $\rho_\infty(T_a)$ are instant and equilibrium ($t \rightarrow \infty$) values of the specific residual electrical resistance at the annealing temperature T_a , $1/\tau_i$ is a reciprocal time of relaxation of the residual electrical resistivity by the i -th relaxation ‘scenario’.

In stationary external conditions, that is, with a constant concentration of defects (vacancies), several models of the kinetics of specific residual electrical resistance can be used.

The simplest is the 1st-order kinetic model:

$$F(\tau^{-1}; \rho(t, T_a) - \rho_\infty(T_a)) \cong \tau^{-1}(\rho(t, T_a) - \rho_\infty(T_a)),$$

where the SRO relaxation kinetics is characterized by the exponential behaviour of the normalized change in the specific residual electrical resistance [5, 53]:

$$\frac{\Delta\rho(t, T_a)}{\Delta\rho_0(T_a)} \cong e^{-t/\tau(T_a)},$$

with the single relaxation time $\tau(T_a)$, which is determined, particularly, by the concentration c_v and the frequency of jumps (mobility) v_v of vacancies with efficiency factor χ ($\tau^{-1} \approx \chi c_v v_v$), where $\Delta\rho(t, T_a) = \rho(t, T_a) - \rho_\infty(T_a)$, $\Delta\rho_0(T_a) = \rho_0(T_a) - \rho_\infty(T_a)$, and $\rho_0(T_a)$ being an initial ($t = 0$) specific residual electrical resistance at the temperature T_a .

In the 2nd-order kinetics model (with the ‘weight’ of the first relaxation ‘scenario’ A),

$$\frac{\Delta\rho(t, T_a)}{\Delta\rho_0(T_a)} \approx A e^{-t/\tau_1(T_a)} + (1 - A) e^{-t/\tau_2(T_a)},$$

the SRO relaxation at the annealing temperature T_a occurs by means of the two relaxation ‘scenarios’ simultaneously with the relaxation times $\tau_1(T_a)$ and $\tau_2(T_a)$.

Thus, the experimental measurement of the specific residual electrical resistance makes it possible to estimate its relaxation times, and, on the contrary, from the relaxation times known from independent (*e.g.*, diffraction) experiments, it is possible to determine the normalized change of the specific residual electrical resistance $\Delta\rho(t, T_a)/\Delta\rho_0(T_a)$ within the framework of one of the two models of its relaxation kinetics.

Note that both models within the diffraction and resistometric methods do not fully describe the kinetics of SRO relaxation. For a more accurate description of it, one should use the 3rd-order kinetics model, which assumes the presence in the expressions for $\Delta I_{\text{diff}}(\mathbf{k}, t)/\Delta I_{\text{diff}}(\mathbf{k}, 0)$ or $\Delta\rho(t, T_a)/\Delta\rho_0(T_a)$ exactly three exponential terms, and therefore, three relaxation times.

Using the measurement of the specific electrical resistance ρ [56, 57] of cast polycrystalline samples in the temperature range from 1273 K to the melting temperature (*i.e.*, 1643 K for the Ni₃Al composition) with quench-

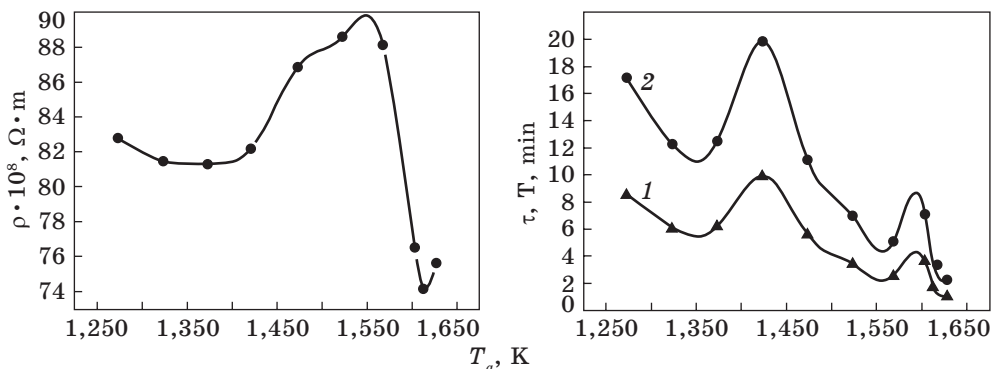


Fig. 2. Annealing-temperature (T_a) dependences of specific residual electrical resistence ρ_∞ in the thermodynamic equilibrium (left) and parameter of the residual resistivity relaxation τ (and T) due to the short-range (or respectively, long-range) ordering within the 1st-order kinetics model for f.c.c.-Ni-24.7 at.% Al after quenching from $T_q \geq 1723$ K (1 — for τ , 2 — for T) [5]

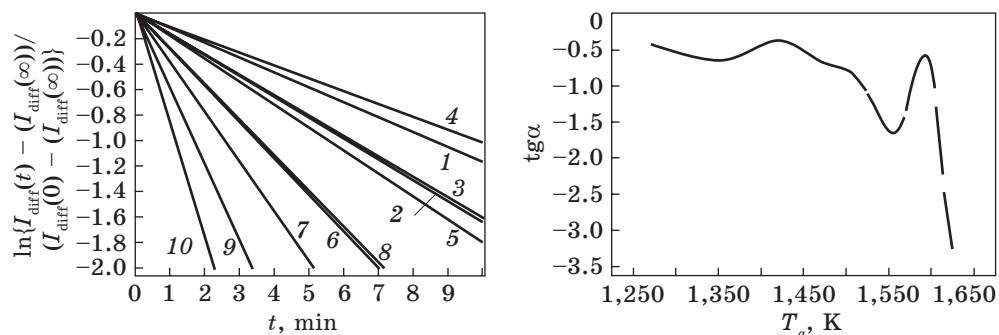
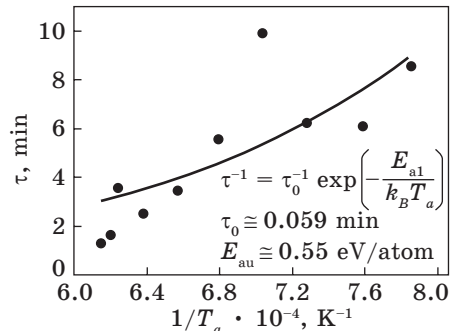


Fig. 3. Time dependences (left) of the normalized change of intensity of diffuse scattering of radiations (at $\mathbf{k} = \mathbf{k}^*$) in Ni-24.7 at.% Al within the 1st-order model for annealing temperatures T_a : 1 — 1273 K, 2 — 1323 K, 3 — 1373 K, 4 — 1423 K, 5 — 1473 K, 6 — 1523 K, 7 — 1568 K, 8 — 1603 K, 9 — 1613 K, 10 — 1624 K (after quenching from $T_q \geq 1723$ K); (right) tangent of angle (α) of a slope of the curve in the left figure to the abscissa axis [5]

ing from temperatures $T_q \geq 1723$ K, the fitting parameters and relaxation times of the residual electrical resistivity were estimated (Fig. 2).

In the assumption of the coincidence of the largest characteristic relaxation times for diffuse scattering of radiations and residual electrical resistivity, the largest characteristic relaxation times for diffuse scattering are estimated. This allowed plotting graphs of the time dependence of the normalized change in the intensity of diffuse scattering of radiations corresponding to that star of wave vector \mathbf{k}^* , which dominates the patterning of the SRO structure at different annealing temperatures for f.c.c.-Ni-24.7 at.% Al, within the framework of the 1st- and 2nd-order kinetics models (Fig. 3).

Fig. 4. Smoothing graph of the dependence of the relaxation time τ of residual resistivity in Ni–24.7 at.% Al on the inverse annealing temperature $1/T_a$ after quenching from $T_q \geq 1723$ K (points are estimated from experimental data) [5]



Neglecting jumps of substitutional atoms outside the first co-ordination sphere, it is possible to estimate the ordering activation energy E_{ao} (which characterizes the elementary act of rearrangement of atomic configurations into an energetically favourable ordered configuration) for the Ni₃Al alloy, considering that it is determined mainly by the value of the migration-activation energy for atoms, E_{al} : $\tau^{-1} = \tau_0^{-1} \exp\{-E_{al}/(k_B T_a)\}$; τ is the relaxation time at annealing temperature T_a , τ_0 is a pre-exponential coefficient. Using the mid-square method, we obtain $E_{ao} \cong E_{al} \cong 0.55$ eV, $\tau_0 \cong 3.544$ s (Fig. 4).

4. Influence of Atomic-Order Relaxation on the Diffuse-Scattering Intensity, Electrical Resistivity, and Microhardness

With the processing of the available experimental data (see Fig. 5 for f.c.c.-Ni–9 at.% Al, as well as for f.c.c.-Ni–6.3 at.% Al in Refs. [60, 61]) within the framework of 1st-, 2nd-, and 3rd-order kinetics models, a number of relaxation parameters were estimated: relaxation times τ_i ($i = 1, 2, 3$) of the diffuse-scattering intensity of x-rays (Tables 1–3) [60, 61] and the corresponding Fourier components of atomic-jump probabilities (per unit of time) (Table 4), as well as specific residual electrical resistance (Tables 5 and 6) and microhardness (μ ; Tables 7 and 8).

Table 1. Parameters of scattering within the 1st-order relaxation kinetics model of diffuse-scattering intensity $I_{\text{SRO}}(\mathbf{k}_X, t)$ for f.c.c.-Ni–6.3 at.% Al [5]

$T_a, \text{ K}$	$I_{\text{SRO}}(t \rightarrow \infty),$ L.un.	$I_{\text{SRO}}(t=0) - I_{\text{SRO}}(t \rightarrow \infty),$ L.un.	$\tau, \text{ h}$	$T, \text{ h}$	\wp^2	δ^2
573	1.12 ± 0.06	-0.31 ± 0.10	9.01 ± 6.85	18.02 ± 13.7	0.71	0.007
673	2.0 ± 0.117	-0.60 ± 0.18	4.58 ± 3.54	9.16 ± 7.08	0.68	0.034
973	1.97 ± 0.012	-0.36 ± 0.03	2.25 ± 0.43	4.50 ± 0.86	0.97	0.001

Table 2. The same as in the previous table, but within the 2nd-order model [5]

$T_a, \text{ K}$	$I_{\text{SRO}}(t \rightarrow \infty), \text{ L.un.}$	$I_{\text{SRO}}(t=0) - I_{\text{SRO}}(t \rightarrow \infty), \text{ L.un.}$	$\tau, \text{ h}$	$T, \text{ h}$	\wp^2	δ^2
573	1.12	-0.31	9.005	9.004	0.71	0.014
673	2.00	-0.60	4.583	4.582	0.68	0.057
973	1.97	-0.36	0.085	4.083	0.99	0.001

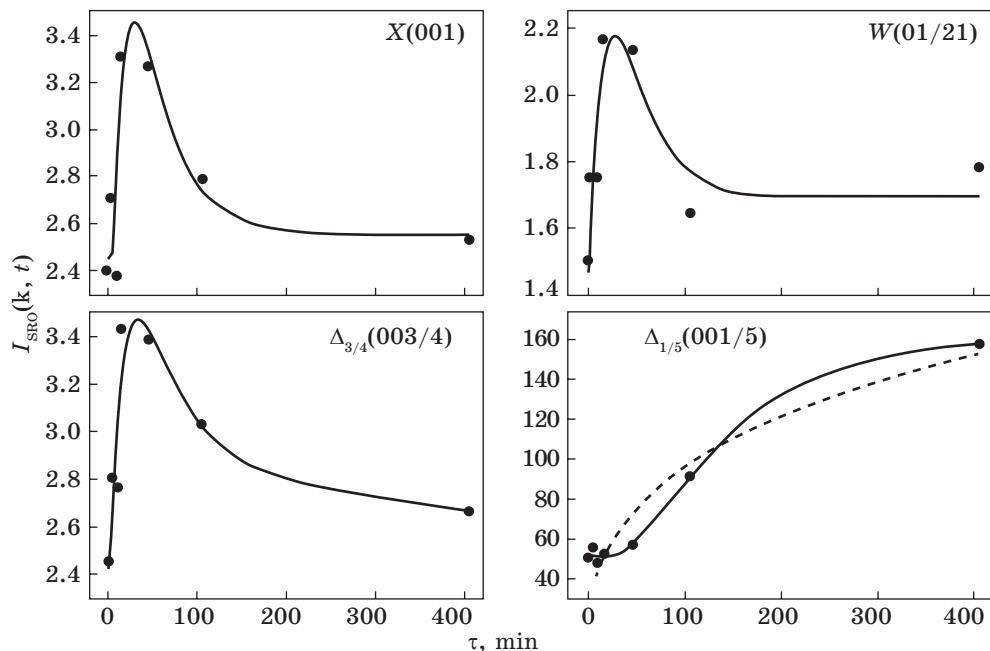


Fig. 5. Kinetics dependences of intensity of diffuse scattering of x-rays (for different positions of the points—ends of wave vector \mathbf{k}) in Ni-9 at.% Al alloy during the annealing at 373 K after quenching from 1073 K. For comparison in the long-wave range (where $\mathbf{k} \cong \Gamma$), which probably corresponds to the coalescence (of clusters, embryos, grains from large distances) at more late stages of annealing, dashed line depicts asymptotic kinetic curve for the coalescence (according to Lifshitz–Slyozov–Wagner theory): $I_{\text{SRO}}(\mathbf{k}, t) \propto t^{1/3}$ [68]

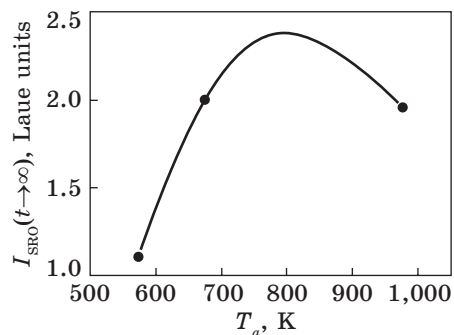


Fig. 6. The annealing-temperature (T_a) dependence of the intensity of diffuse scattering $I_{\text{SRO}}(t \rightarrow \infty)$ in the thermodynamic equilibrium calculated within the 1st-order kinetics model for Ni-6.3 at.% Al alloy [5]

So, for the 1st-order kinetics model, ρ_∞ , $P_0 - \rho_\infty$, τ , *etc.* are desired parameters (Table 5, where $T \cong 2\tau$ is a rough estimate of long-range atomic-order relaxation by the exchange mechanism). In the case of the 2nd-order model, the desired parameters are ρ_∞ , $P_0 - \rho_\infty$, A , τ_1 , τ_2 , *etc.* (Table 6). Since the number of independent fitting parameters increases as $3n - 1$, to ensure the reliability of the analysis, the number of exponential terms (n) required for fitting the data, as a rule, should not exceed 2 or 3.

The criteria for the correspondence of such graphs (Figs. 6–14) to the experimental points can be determined by the small value of the root-mean-square deviation δ^2 and the correlation coefficient \wp (Tables 1–8).

Table 3. The same as in the previous table, but for f.c.c.-Ni-9 at.% Al within the 3rd-order model ($\tau_3 = 2\tau_1\tau_2/2(\tau_1 + \tau_2)$, $T_q = 1073$ K, $T_a = 373$ K) [60]

k	$I_{\text{SRO}}(\mathbf{k}, \infty)$	$A_1(\mathbf{k})$	$A_2(\mathbf{k})$	$A_3(\mathbf{k})$	$\tau_1(\mathbf{k})$, h	$\tau_2(\mathbf{k})$, h	$\tau_3(\mathbf{k})$, h
X(0 0 1)	2.55	3.50	2.59	-6.19	0.101	0.680	0.176
W(0 1/2 1)	1.70	-122.9	201.4	-78.67	0.389	0.393	0.391
$\Delta_{3/4}(0 0 3/4)$	2.55	-3.31	0.50	2.74	0.328	6.194	0.623
$\Delta_{1/5}(0 0 1/5)$	161.85	-55.00	-206.8	151.5	0.286	1.720	0.491

Table 4. Fourier components (with an opposite sign) of probabilities of atomic jumps (per unit of time) $\lambda_1(\mathbf{k})$, $\lambda_2(\mathbf{k})$, $\lambda_3(\mathbf{k}) = \lambda_1(\mathbf{k}) + \lambda_2(\mathbf{k})$ for f.c.c.-Ni-9 at.% Al ($T_q = 1073$ K, $T_a = 373$ K) within the 3rd-order model [60]

k	$\lambda_1(\mathbf{k}) \times 10^5$, s ⁻¹	$\lambda_2(\mathbf{k}) \times 10^5$, s ⁻¹	$\lambda_3(\mathbf{k}) \times 10^5$, s ⁻¹
X(0 0 1)	137.51	20.44	157.95
W(0 1/2 1)	35.70	35.37	71.07
$\Delta_{3/4}(0 0 3/4)$	42.32	2.24	44.56
$\Delta_{1/5}(0 0 1/5)$	48.51	8.08	56.59

Table 5. Fitting parameters of relaxation calculated within the 1st-order relaxation kinetics model of residual electrical resistivity for f.c.c.-Ni-6.3 at.% Al [5]

T_a , K	ρ_∞/ρ_0	$(\rho_0 - \rho_\infty)/\rho_0$	τ , h	T, h	\wp^2	δ^2
573	1.025 ± 0.001	-0.026 ± 0.002	1.07 ± 0.19	2.13	0.97	3.61×10^{-6}

Table 6. The same as in the previous table, but for the 2nd-order model [5, 61]

T_a , K	ρ_∞/ρ_0	$(\rho_0 - \rho_\infty)/\rho_0$	τ_1 , h	τ_2 , h	\wp^2	δ^2
573	1.03 ± 0.001	-0.141	1.067	1.064	0.97	5.1×10^{-6}
673	1.01 ± 0.0001	-0.006	0.904	0.903	0.95	3.2×10^{-6}

Table 7. Relaxation parameters calculated within the 1st-order kinetics model for relaxation of microhardness of f.c.c.-Ni-6.3 at.% Al [5, 61]

T_a , K	μ_∞ , kg/mm ²	$\mu_0 - \mu_\infty$, kg/mm ²	τ , h	T, h	\wp^2	δ^2
573	239.15 ± 1.36	-32.17 ± 3.73	0.52 ± 0.13	1.04 ± 0.26	0.90	13.77

Table 8. The same as in the previous table but within the 2nd-order relaxation kinetics model [5, 61]

T_a , K	μ_∞ , kg/mm ²	$\mu_0 - \mu_\infty$, kg/mm ²	τ_1 , h	τ_2 , h	\wp^2	δ^2
573	239.15	-32.17	0.521	0.521	0.90	17.705
673	210.58	-11.37	0.960	0.966	0.94	4.049

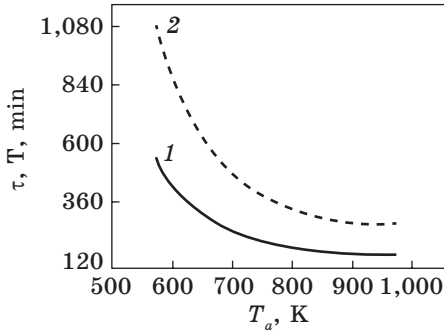


Fig. 7. The annealing-temperature (T_a) dependence of estimated relaxation times of short-range (1 — τ) and long-range (2 — T) orders in the 1st-order kinetics model for Ni-6.3 at.% Al [5]

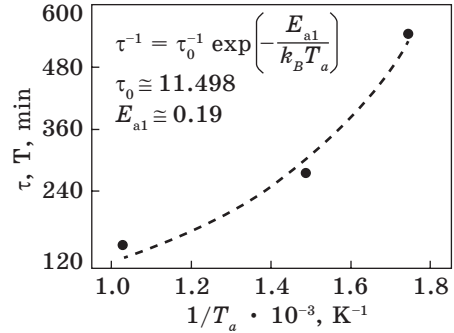


Fig. 8. The relaxation time τ of SRO vs. the inverse annealing temperature T_a^{-1} estimated within the 1st-order kinetics model for Ni-6.3 at.% Al [5]

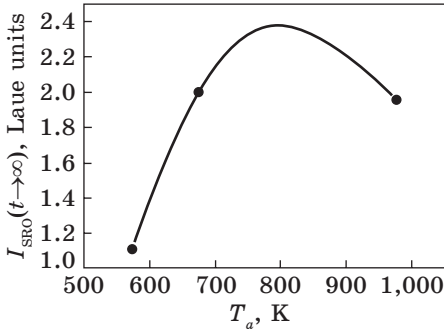


Fig. 9. The diffuse-scattering intensity $I_{\text{SRO}}(t \rightarrow \infty)$ in the thermodynamic equilibrium vs. the annealing temperature T_a within the 2nd-order kinetics model for Ni-6.3 at.% Al [5]

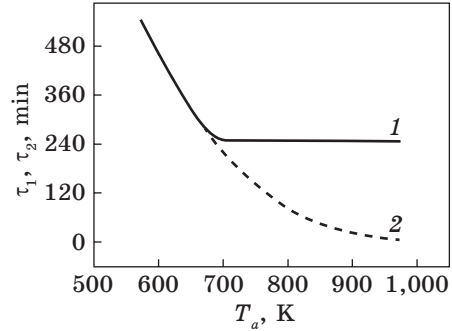


Fig. 10. Relaxation parameters τ_1 (1) and τ_2 (2) estimated within the 2nd-order model vs. the annealing temperature T_a for Ni-6.3 at.% Al [5]

Results in Table 1 and the dependence $\tau^{(p)} \cong \tau_0 \exp\{E_{a1}/(k_B T_a^{(p)})\}$ ($p = 1, 2, 3$) allow estimation of the activation energy of the jump-like atomic movement in the low-concentration f.c.c.-Ni-6.3 at.% Al alloy (here, $\tau^{(p)}$ is a relaxation time presenting p -th annealing temperature $T_a^{(p)}$; τ_0 is a pre-exponential coefficient; $E_{a1} \cong E_m$ is an activation energy of elementary jump of an atom into the vacancy).

For the 1st-order kinetics model, $E_{a1} \cong 0.19$ eV/atom, $\tau_0 \cong 689.9$ s. For comparison, the rough estimation [62, 63] of the activation energy in the intermetallic Ni₃Al is $E_{a_0} \cong 0.55$ eV/atom (for the exchange mechanism of atomic diffusion during the atomic long-range order relaxation at 1273–1626 K).

The influence of SRO on the mechanical properties of the alloy is

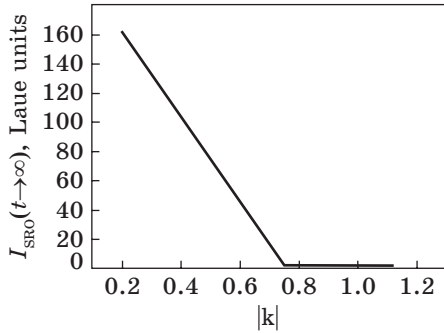


Fig. 11. The diffuse-scattering intensity in the thermodynamic equilibrium within the 3rd-order model vs. the position of the end of wave vector \mathbf{k} for Ni-9 at.% Al [5]

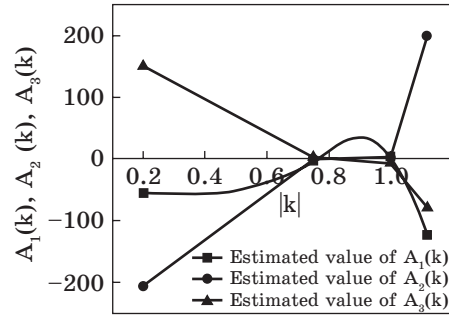


Fig. 12. Predicted dependences of pre-exponential coefficients $A_1(\mathbf{k})$, $A_2(\mathbf{k})$, and $A_3(\mathbf{k})$ estimated within the 3rd-order atomic-ordering kinetics model on the position of the end of wave vector \mathbf{k} for f.c.c.-Ni-9 at.% Al ($T_q = 1073$ K and $T_a = 373$ K) [5]

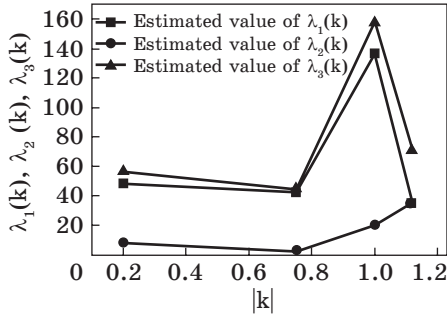


Fig. 13. The dependences of Fourier components of probabilities of atomic jumps on the position of wave vector \mathbf{k} within the 3rd-order kinetics model for f.c.c.-Ni-9 at.% Al ($T_q = 1073$ K and $T_a = 373$ K) [5]

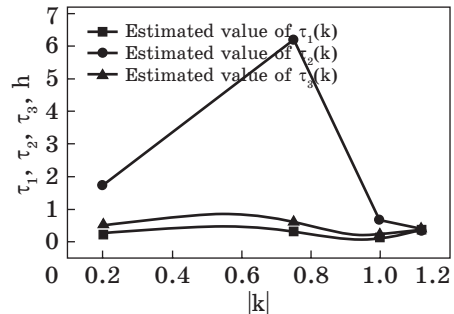


Fig. 14. Predicted dependences of relaxation time parameters τ_1 , τ_2 , and τ_3 ($\tau_3 = 2\tau_1\tau_2/(\tau_1 + \tau_2)$) on the position of wave vector \mathbf{k} within the 3rd-order kinetics model for f.c.c.-Ni-9 at.% Al ($T_q = 1073$ K and $T_a = 373$ K) [5]

caused by the two main factors. First, the movement of dislocations during deformation destroys SRO with additional energy absorption, which also determines additional strengthening. Second, changes in the total energy of the alloy and its electronic structure due to the appearance of SRO are regulated by the elastic or plastic deformations in an alloy with SRO in a different way than in the same alloy without SRO. The microhardness of the Ni-6.3 at.% Al alloy changes nonmonotonically during annealing at 573 and 673 K, but it increases because of the occurrence of local order [58].

Due to the complexity of SRO transformations in Ni-Al, the modeling of its local atomic configurations is also of interest. Computer modeling of the SRO structure in the Ni-9 at.% Al solid solution was per-

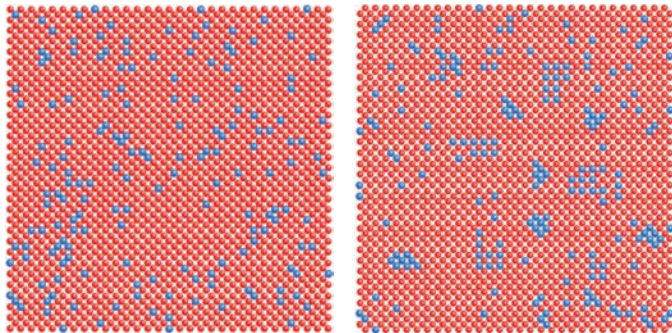


Fig. 15. Monte Carlo method modelling of short-range ordering in Ni-9 at.% Al for random distribution of components (left) and after quenching from 1073 K with further annealing at 373 K for 15 min (right) [60, 61]

formed by the Monte Carlo method using the experimentally obtained values of the Warren–Cowley SRO parameters α_{klm} . The simulation was performed for a three-dimensional array with 2.16×10^5 sites of the f.c.c. lattice with cyclic boundary conditions. For alloy with 9 at.% of Al, 19440 sites were corresponded to alloying Al atoms. Initially, a random distribution of atoms was generated (Fig. 15, left). It can be seen that such a distribution lacks any features of local spatial interatomic correlations. Then, randomly chosen Ni and Al atoms exchanged their locations, and further, the parameter $\Delta = \sum_{klm} (\alpha_{klm}^{\text{calc}} - \alpha_{klm}^{\text{exp}})^2 / \sum_{klm} (\alpha_{klm}^{\text{exp}})^2$ was calculated after each atomic rearrangement, where $\alpha_{klm}^{\text{exp}}$ and $\alpha_{klm}^{\text{calc}}$ are experimental and calculated Warren–Cowley SRO parameters, respectively. If the value of Δ decreased, then, the atoms of both types remained in new places, and if it did not decrease, then, they returned to their original positions, but only $\Delta \leq 10^{-6}$ were taken into account.

Figure 15 (right) exhibits the atomic distribution for the SRO state in Ni-9 at.% Al quenched from 1073 K and further annealed at 373 K for 15 min. As seen, after the isothermal annealing for 15 min, there are some clusters ordered as the $L1_2$ -type (Ni_3Al), as well as regions with short-range decomposition. The SRO modelling performed for Ni-9 at.% Al confirms the presence in the alloy of several concentration waves [4] with different wave vectors \mathbf{k}_s , which dominate the representation of the SRO structure.

The study of the kinetics of initiation of an equilibrium SRO within the f.c.c.-Ni-Al alloy shows that this process possesses a relaxation nature and is carried out through the diffusion of Ni ions in a ‘coat’ of Al ions. As shown, the rate of this process is different for different points of the reciprocal space. The obtained data on the SRO-relaxation rate for various points of the reciprocal space are evidence in favour of not only the traditional vacancy mechanism of diffusion (with atoms’ jumpings into the nearest vacancies). The same data can be used to determine the probability of jumps of Ni ions in elementary acts of diffusion. Such acts are performed mainly as jumps not only at the nearest distance. However, the probability of Ni-ions’ jumpings to the \mathbf{R} site from its nearest sites is

greater for those **R** sites, in which the presence of Ni ions is energetically more advantageous. Thus, the probability of intersite ionic jumps depends on the distribution of the ‘potential’ field caused by the SRO and, therefore, on the alloy imperfection.

Thus, we studied the time dependence of the diffuse scattering of both x-rays and conductivity electrons (electrical resistivity), which is attributed to establishing an equilibrium SRO in the relaxation process of isothermal annealing. As found, during long-term annealing of a single-phase alloy, the intermediate concentration inhomogeneities (which differ from the $L1_2$ -type SRO state and are formed already at the initial annealing stages) appear. Their appearance is accompanied by a drop in the diffuse-scattering intensity in the superstructure points of the lattice reciprocal space.

5. Conclusions

By parameterizing the literature data on the measurement of residual electrical resistivity during isothermal annealing of substitutional f.c.c.-Ni–Al alloys within the framework of the proposed models of atomic-order relaxation kinetics, the most characteristic relaxation times of residual electrical resistivity after quenching and its equilibrium values for these alloys at different annealing temperatures were estimated.

The maximum characteristic relaxation time of the atomic order of such alloys was determined and, based on the hypothesis of the coincidence of the largest characteristic relaxation times (for the same reasons) of the intensity of diffuse scattering of radiations and the residual electrical resistivity, curves of the time dependence of the normalized change in the intensity of diffuse scattering of rays were predicted, which correspond to the wave-vector star that generates the type of the SRO structure, at different annealing temperatures.

As found, the temperature dependence of the equilibrium residual electrical resistivity of concentrated f.c.c.-Ni–Al alloys has a pronounced nonmonotonic character, which is due not only to the scattering of electrons by nonlocalized excitations (*e.g.*, magnons, *etc.*), but also mainly to their scattering by substitutional point defects, which are redistributed, observing the SRO, but differently depending on the annealing temperature: from atomic configurations in the close environment, which on average resemble substitution by the superstructural $L1_2$ type, to configurations of the environment corresponding to the superstructural $L1_0$ type, or clusters of identical atoms. Such an explanation requires a significant modification of the existing models for the electrical conductivity of the indicated alloys (in particular, taking into account differences in the scattering of conductivity electrons with different spin projections on certain excitations or distortions, the structure of which is sensitive to temperature changes) [64–67]).

The nonmonotonic temperature dependence of the estimated relaxation time of the residual electrical resistivity for the concentrated f.c.c. Ni–Al alloy has a pronounced non-Arrhenius character and is due to a diffusion rearrangement of the SRO not only by jumps of Al and Ni atoms into the sites of the first co-ordination sphere around them, but also by jumps of these substitutional atoms beyond its boundaries. Such an explanation also requires a significant modification of the already proposed models of the transport characteristics of alloys.

The slope of the line of the predicted time dependence of the logarithm of the difference between the instant and equilibrium intensities of diffuse scattering of rays (in the vicinity of the wave vector that generates the type of SRO structure) relative to the time axis changes nonmonotonically with increasing annealing temperature.

Within the framework of the applied 1st- and 2nd-order kinetic models, the largest characteristic relaxation times of the residual electrical resistivity and microhardness after quenching, as well as their equilibrium values for low-concentration f.c.c.-Ni–Al alloys at different annealing temperatures, were estimated. The maximum characteristic relaxation time of the atomic order of such alloys was predicted and the time dependence curves of the normalized change in the intensity of diffuse scattering of rays, corresponding to the wave-vector star that dominates in the reflection of the atomic-order structure, were predicted at different annealing temperatures for these alloys.

The SRO relaxation to the equilibrium state for f.c.c.-Ni–Al solid solution is accompanied by the transformation of its initial type into short-range ordering as a whole, and the relative number of clusters in the formed structure increases with time. This is consistent with the results of computer simulations of local atomic ordering by the Monte Carlo method and the inhomogeneous SRO model.

Acknowledgements. Authors are grateful to the National Research Foundation of Ukraine (NRFU) for grant support of the project ‘Durability Enhancement of Aircraft Metal Materials: Formation of Structural-Phase States and Physical-Mechanical Properties as Affected by the Solid-Solution, Dispersion and Work Hardenings, and Surface Finishing’ (State Reg. No. 0123U103378) within the NRFU Competition ‘Science for the Recovery of Ukraine in the War and Post-War Periods’ (application ID 2022.01/0038; agreements Nos. 161-0038 as of 01.08.2023 and 41-0038 as of 01.03.2024). We are obliged to the Armed Forces of Ukraine for providing security made possible to perform this work as a part of the mentioned project.

REFERENCES

1. A.G. Khachatryan, *Fiz. Tverd. Tela*, **9**, No. 9: 2594 (1967) (in Russian).
2. A.G. Khachatryan, *Fiz. Tverd. Tela*, **11**, No. 12: 3534 (1969) (in Russian).

3. M.A. Krivoglaz, *Zh. Eksp. Tepr. Fiz.*, **40**, No. 6: 1812 (1961) (in Russian).
4. A.G. Khachatryan, *Theory of Structural Transformations in Solids* (Mineola, NY: Dover Publications, Inc.: 2008).
5. V.A. Tatarenko, O.V. Sobol', D.S. Leonov, Yu.A. Kunyts'kyy, and S.M. Bokoch, Statistical thermodynamics and physical kinetics of structural changes of quasi-binary solid solutions based on the close-packed simple lattices (according to the data about evolution of a pattern of scattering of waves of various kinds), *Usp. Fiz. Met.*, **12**, No. 1: 1 (2011) (in Ukrainian);
<https://doi.org/10.15407/ufm.12.01.001>
6. L.S. Darken, *AIME Transactions*, **175**: 184 (1948).
7. M.A. Krivoglaz, *Theory of X-Ray and Thermal Neutron Scattering by Real Crystals* (New York: Springer: 1969).
8. H.E. Cook, The kinetics of clustering and short-range order in stable solid solutions, *J. Phys. Chem. Solids*, **30**, No. 10: 2427 (1969);
[https://doi.org/10.1016/0022-3697\(69\)90067-5](https://doi.org/10.1016/0022-3697(69)90067-5)
9. P.R. Okamoto and G. Thomas, On short range order and micro-domains in the Ni₄Mo system, *Acta Metall.*, **19**, No. 8: 825 (1971);
[https://doi.org/10.1016/0001-6160\(71\)90139-8](https://doi.org/10.1016/0001-6160(71)90139-8)
10. S.K. Das, P.R. Okamoto, P.M.J. Fischer, and G. Thomas, Short range order in Ni–Mo, Au–Cr, Au–V and Au–Mn alloys, *Acta Metall.*, **21**, No. 7: 913 (1971).
11. S. Hata, H. Fujita, C.G. Schlesier, S. Matsumura, N. Kuwano, and K. Oki, *Materials Transaction: The Jpn. Institute of Metals*, **39**, No. 1: 133 (1998);
<https://doi.org/10.2320/matertrans1989.39.133>
12. S. Hata, S. Matsumura, N. Kuwano, K. Oki, and D. Shindo, *Acta Mater.*, **46**, No. 14: 4955 (1998);
[https://doi.org/10.1016/S1359-6454\(98\)00180-3](https://doi.org/10.1016/S1359-6454(98)00180-3)
13. S. Hata, D. Shindo, N. Kuwano, S. Matsumura, and K. Oki, Monte Carlo study of ordering processes in fcc-based Ni–Mo Alloys, *Materials Transaction: The Jpn. Institute of Metals*, **39**, No. 9: 914 (1998);
<https://doi.org/10.2320/matertrans1989.39.914>
14. S. Hata, D. Shindo, T. Mitate, N. Kuwano, S. Matsumura, and K. Oki, HRTEM image contrast of short range order in Ni₄Mo, *Micron*, **31**, No. 5: 533 (2000);
[https://doi.org/10.1016/S0968-4328\(99\)00134-1](https://doi.org/10.1016/S0968-4328(99)00134-1)
15. S. Hata and S. Matsumura, 合金の短範囲規則状態の微視的構造, *The Crystallographic Society of Jpn.*, **44**, No. 4: 225 (2002);
<https://doi.org/10.5940/jcrsj.44.225>
16. D. de Fontaine, k-space symmetry rules for order–disorder reactions, *Acta Metall.*, **23**, No. 5: 553 (1975);
[https://doi.org/10.1016/0001-6160\(75\)90096-6](https://doi.org/10.1016/0001-6160(75)90096-6)
17. H.E. Cook, Continuous transformations, *Mater. Sci. Eng.*, **25**: 127 (1976);
[https://doi.org/10.1016/0025-5416\(76\)90059-8](https://doi.org/10.1016/0025-5416(76)90059-8)
18. D. de Fontaine, *Solid State Physics* (Eds. H. Ehrenreich, F. Seits, and D. Turnbull) (New York: Academic Press.: 1979), vol. **34**, p. 73.
19. H. Chen and J.B. Cohen, Measurements of the ordering instability in binary alloys, *Acta Metall.*, **27**, No. 2: 603 (1979);
[https://doi.org/10.1016/0001-6160\(79\)90012-9](https://doi.org/10.1016/0001-6160(79)90012-9)
20. H. Chen and J.B. Cohen, Pretransition phenomena in first-order order–disorder transitions, *Metallurg. Mater. Trans. A*, **12**, No. 4: 575 (1981);
<https://doi.org/10.1007/BF02649731>
21. U.D. Kulkarni and S. Banerjee, Phase separation during the early stages of ordering

- in Ni_3Mo , *Acta Metall.*, **36**, No. 2: 413 (1998);
[https://doi.org/10.1016/0001-6160\(88\)90017-X](https://doi.org/10.1016/0001-6160(88)90017-X)
22. S. Banerjee, U.D. Kulkarni, and K. Urban, Initial stages of ordering in Ni_3Mo — thermal and irradiation ordering experiments, *Acta Metall.*, **37**, No. 1: 35 (1989);
[https://doi.org/10.1016/0001-6160\(89\)90264-2](https://doi.org/10.1016/0001-6160(89)90264-2)
23. A. Arya, S. Banerjee, G.P. Das, I. Dasgupta, T. Saha-Dasgupta, and A. Mookerjee, A first-principles thermodynamic approach to ordering in Ni–Mo alloys, *Acta Mater.*, **49**, No. 17: 3575 (2001);
[https://doi.org/10.1016/S1359-6454\(01\)00235-X](https://doi.org/10.1016/S1359-6454(01)00235-X)
24. A. Arya, G.K. Dey, V.K. Vasudevan, and S. Banerjee, Effect of chromium addition on the ordering behaviour of Ni–Mo alloy: experimental results vs. electronic structure calculations, *Acta Mater.*, **50**, No. 14: 3301 (2002);
[https://doi.org/10.1016/S1359-6454\(02\)00093-9](https://doi.org/10.1016/S1359-6454(02)00093-9)
25. A. Mookerjee, T. Saha-Dasgupta, I. Dasgupta, A. Arya, S. Banerjee, and G.P. Das, A first-principles thermodynamic approach to ordering in binary alloys, *Bulletin of Materials Science*, **26**, No. 1: 79 (2003);
<https://doi.org/10.1007/BF02712791>
26. H.E. Cook, Brownian motion in spinodal decomposition, *Acta Metall.*, **18**, No. 3: 297 (1970);
[https://doi.org/10.1016/0001-6160\(70\)90144-6](https://doi.org/10.1016/0001-6160(70)90144-6)
27. H.E. Cook, D. de Fontaine, and J.E. Hillard, A model for diffusion on cubic lattices and its application to the early stages of ordering, *Acta Metall.*, **17**, No. 6: 765 (1969);
[https://doi.org/10.1016/0001-6160\(69\)90083-2](https://doi.org/10.1016/0001-6160(69)90083-2)
28. V.A. Tatarenko and T.M. Radchenko, Parameters of the short-range order relaxation kinetics and interactions of atoms in binary substitutional f.c.c. solid solutions from the data of time evolution of diffuse scattering of radiation, *Metallofiz Noveishie Tekhnol.*, **24**, No. 10: 1335 (2002).
29. S.M. Bokoch, N.P. Kulish, T.M. Radchenko, S.P. Repetskij, and V.A. Tatarenko, Parameters of a relaxation of an electrical resistance and diffuse scattering in binary substitutional solutions fcc-Ni–Mo, *Metallofiz. Noveishie Tekhnol.*, **24**, No. 5: 691 (2002) (in Russian).
30. M.M. Naumova, S.V. Semenovskaya, and Ya.S. Umanskiy, *Fiz. Tverd. Tela*, **12**, No. 4: 976 (1970) (in Russian).
31. F. Bley, Z. Amilius, and S. Lefebvre, Wave vector dependent kinetics of short-range ordering in $62\text{Ni}_0.765\text{Fe}_0.235$, studied by neutron diffuse scattering, *Acta Metall.*, **36**, No. 7: 1643 (1988);
[https://doi.org/10.1016/0001-6160\(88\)90231-3](https://doi.org/10.1016/0001-6160(88)90231-3)
32. M.M. Naumova and S.V. Semenovskaya, *Fiz. Tverd. Tela*, **13**, No. 12: 3632 (1970) (in Russian).
33. H. Chen and J. Cohen, A comparison of experiment and the theory of continuous ordering, *Supplément au J. de Physique Colloques*, **38**, No. 7: 314 (1977);
<https://doi.org/10.1051/jphyscol:1977762>
34. S. Banerjee, K. Urban, and M. Wilkens, Order–disorder transformation in Ni_4Mo under electron irradiation in a high-voltage electron microscope, *Acta Metall.*, **32**, No. 3: 299 (1984); [https://doi.org/10.1016/0001-6160\(84\)90103-2](https://doi.org/10.1016/0001-6160(84)90103-2)
35. S.M. Bokoch, M.P. Kulish, T.M. Radchenko, and V.A. Tatarenko, Kinetics of short-range ordering of substitutional solid solutions (according to data on a scattering of various kinds of waves). I. Microscopic parameters of migration of atoms within f.c.c.-Ni–Mo in Fourier-representation, *Metallofiz. Noveishie Tekhnol.*, **26**,

- No. 3: 387 (2004) (in Russian).
36. T.M. Radchenko and V.A. Tatarenko, Fe–Ni alloys at high pressures and temperatures: statistical thermodynamics and kinetics of the $L1_2$ or DO_{19} atomic order, *Usp. Fiz. Met.*, **9**, No. 1: 1 (2008) (in Ukrainian); <https://doi.org/10.15407/ufm.09.01.001>
 37. T.M. Radchenko, V.A. Tatarenko, S.M. Bokoch, and M.P. Kulish, Microscopic approach to the evaluation of diffusion coefficients for substitutional f.c.c. solid solutions, *Proc. of the 1st Int'l Conf. on Diffusion in Solids and Liquids—'DSL-2005'* (Aveiro, Portugal, 6–8 July, 2005) (Eds. A. Öchsner, J. Grácio, and F. Barlat) (Aveiro: University of Aveiro: 2005), vol. 2, p. 591.
 38. S.M. Bokoch, M.P. Kulish, V.A. Tatarenko, and T.M. Radchenko, Kinetics of short-range ordering of substitutional solid solutions (according to data on a scattering of various kinds of waves). II. Parameters of atomic microdiffusion within f.c.c.-Ni–Mo, *Metallofiz. Noveishie Tekhnol.*, **26**, No. 4: 541 (2004) (in Russian).
 39. V.A. Tatarenko and T.M. Radchenko, The application of radiation diffuse scattering to the calculation of phase diagrams of f.c.c. substitutional alloys, *Intermetallics*, **11**, Nos. 11–12: 1319 (2003); [https://doi.org/10.1016/S0966-9795\(03\)00174-2](https://doi.org/10.1016/S0966-9795(03)00174-2)
 40. V.A. Tatarenko, T.M. Radchenko, and V.M. Nadutov, Parameters of interatomic interaction in a substitutional alloy f.c.c. Ni–Fe according to experimental data about the magnetic characteristics and equilibrium values of intensity of a diffuse scattering of radiations, *Metallofiz. Noveishie Tekhnol.*, **25**, No. 10: 1303 (2003) (in Ukrainian).
 41. L.-Q. Chen and A.G. Khachaturyan, Formation of virtual ordered states along a phase-decomposition path, *Phys. Rev. B*, **44**, No. 9: 4681 (1991); <https://doi.org/10.1103/PhysRevB.44.4681>
 42. L.-Q. Chen and A.G. Khachaturyan, *Kinetics of Ordering Transformations in Metals* (Eds. H. Chen and V.K. Vasudevan) (Warrendale, Pennsylvania: TMS: 1992), p. 197.
 43. L.-Q. Chen and A.G. Khachaturyan, Kinetics of virtual phase formation during precipitation of ordered intermetallics, *Phys. Rev. B*, **46**, No. 10: 5899 (1992); <https://doi.org/10.1103/PhysRevB.46.5899>
 44. R. Poduri and L.-Q. Chen, Computer simulation of the kinetics of order–disorder and phase separation during precipitation of δ' (Al_3Li) in Al–Li alloys, *Acta Mater.*, **45**, No. 1: 245 (1997); [https://doi.org/10.1016/S1359-6454\(96\)00137-1](https://doi.org/10.1016/S1359-6454(96)00137-1)
 45. R. Poduri and L.-Q. Chen, *Acta Mater.*, **46**, No. 5: 1719 (1998); [https://doi.org/10.1016/S1359-6454\(97\)00335-2](https://doi.org/10.1016/S1359-6454(97)00335-2)
 46. Y. Wang, D. Banerjee, C.C. Su, and A.G. Khachaturyan, Computer simulation of atomic ordering and compositional clustering in the pseudobinary Ni_3Al – Ni_3V system, *Acta Mater.*, **46**, No. 9: 2983 (1998); [https://doi.org/10.1016/S1359-6454\(98\)00015-9](https://doi.org/10.1016/S1359-6454(98)00015-9)
 47. G. Rubin and A.G. Khachaturyan, Three-dimensional model of precipitation of ordered intermetallics, *Acta Mater.*, **47**, No. 7: 1995 (1999); [https://doi.org/10.1016/S1359-6454\(99\)00107-X](https://doi.org/10.1016/S1359-6454(99)00107-X)
 48. V.A. Tatarenko and T.M. Radchenko, Diffusive relaxation of short-range order parameters and the time evolution of diffuse radiation scattering in solid solutions, *Defect Diffus. Forum*, **194–199**, Pt. 1: 183 (2001); <https://doi.org/10.4028/www.scientific.net/DDF.194-199.183>
 49. V.A. Tatarenko, S.M. Bokoch, V.M. Nadutov, T.M. Radchenko, and Y.B. Park,

- Semi-empirical parameterization of interatomic interactions and kinetics of the atomic ordering in Ni–Fe–C permalloys and elinvars, *Defect Diffus. Forum*, **280–281**: 29–78 (2008);
<https://doi.org/10.4028/www.scientific.net/DDF.280-281.29>
50. E.P. Feldman, L.I. Stefanovich, and K.V. Gumennik, *Izv. RAN. Ser.: Fiz.*, **70**: 1048 (2006) (in Russian).
51. T.M. Radchenko and V.A. Tatarenko, Atomic-ordering kinetics and diffusivities in Ni–Fe permalloy, *Defect Diffus. Forum*, **273–276**: 525 (2008);
<https://doi.org/10.4028/www.scientific.net/DDF.273-276.525>
52. T.M. Radchenko, V.A. Tatarenko, and S.M. Bokoch, Diffusivities and kinetics of short-range and long-range orderings in Ni–Fe permalloys, *Metallofiz. Noveishie Tekhnol.*, **28**, No. 12: 1699 (2006).
53. V.A. Tatarenko and T.M. Radchenko, Direct and indirect methods of the analysis of interatomic interaction and kinetics of a relaxation of the short-range order in close-packed substitutional (interstitial) solid solutions, *Usp. Fiz. Met.*, **3**, No. 2: 111 (2002) (in Ukrainian);
<https://doi.org/10.15407/ufm.03.02.111>
54. V.A. Tatarenko, T.M. Radchenko, A.Yu. Naumuk, and B.M. Mordyuk, Statistical-thermodynamic models of the Ni–Al-based ordering Phases ($L1_2$, $L1_0$, $B2$): role of magnetic Ni-atoms' contribution, *Prog. Phys. Met.*, **25**, No. 1: 3 (2024);
<https://doi.org/10.15407/ufm.25.01.003>
55. N.S. Stoloff, Physical and mechanical metallurgy of Ni₃Al and its alloys, *Int. Mater. Rev.*, **34**, No. 4: 153 (1989);
<https://doi.org/10.1179/imr.1989.34.1.153>
56. O.V. Savin, N.N. Stepanova, Yu.N. Akshentsev, B.A. Baum, B.A. Sazonova, and Yu.E. Turhan, *Fiz. Met. Metalloved.*, **88**, No. 4: 69 (1999) (in Russian).
57. O.V. Savin, N.N. Stepanova, Yu.N. Akshentsev, B.A. Baum, and E.E. Baryshev, *Fiz. Met. Metalloved.*, **90**, No. 1: 66 (2000) (in Russian).
58. A.A. Katsnelson and P.Sh. Dazhaev, *Izv. VUZov SSSR. Ser.: Fiz.*, No. 4: 23 (1970) (in Russian).
59. A.A. Katsnelson, A.M. Silonov, and V.M. Silonov, *Fiz. Met. Metalloved.*, **33**, No. 6: 1267 (1972) (in Russian).
60. S.M. Bokoch, D.S. Leonov, M.P. Kulish, V.A. Tatarenko, and Yu.A. Kunitsky, Influence of relaxation of the atomic order in f.c.c.-Ni–Al alloys on X-ray diffuse scattering, *phys. status solidi A*, **206**, No. 8: 1766 (2009);
<https://doi.org/10.1002/pssa.200881604>
61. S.M. Bokoch, D.S. Leonov, M.P. Kulish, V.A. Tatarenko, and Yu.A. Kunitsky, Influence of a relaxation of the atomic order in fcc-Ni–Al alloys on X-ray diffuse scattering, electrical resistance and microhardness, *Metallofiz. Noveishie Tekhnol.*, **30**, No. 12: 1677 (2008).
62. D.S. Leonov, T.M. Radchenko, V.A. Tatarenko, and Yu.A. Kunitskiy, Kinetics parameters of atomic migration and diffuse scattering of radiations within the f.c.c.-Ni–Al alloys, *Defect Diffus. Forum*, **273–276**: 520 (2008);
<https://doi.org/10.4028/www.scientific.net/DDF.273-276.520>
63. D.S. Leonov, T.M. Radchenko, V.A. Tatarenko, and Yu.A. Kunitsky, Kinetic parameters of migration of atoms and relaxation of scattering of different-type waves in the ordering fcc-Ni–Al alloy, *Metallofiz. Noveishie Tekhnol.*, **29**, No. 12: 1587 (2007) (in Russian).
64. V.V. Lizunov, I.M. Melnyk, T.M. Radchenko, S.P. Repetsky, V.A. Tatarenko, Influence of strong electron–electron correlations on the electrical conduction and

- magnetic properties of substitutional alloys as advanced functional spintronic materials, *Functional Magnetic and Spintronic Nanomaterials, NATO Science for Peace and Security Series B: Physics and Biophysics* (Eds. I. Vladymyrskyi, B. Hillebrands, A. Serha, D. Makarov, and O. Prokopenko) (Dordrecht: Springer: 2024), Ch. 1, p. 1;
https://doi.org/10.1007/978-94-024-2254-2_1
65. E.G. Len, I.M. Melnyk, S.P. Repetsky, V.V. Lizunov, and V.A. Tatarenko, Electronic structure and temperature dependence of the linear size of the nanoscale magnetic domains in a disordered bcc-Fe–Co alloy, *Materialwiss. Werkstofftech.*, **42**, No. 1: 47 (2011);
<https://doi.org/10.1002/mawe.201100729>
66. S.P. Repetsky, E.G. Len, and V.V. Lizunov, Energy spectrum of electrons and magnetic susceptibility of Fe–Co alloy, *Metallofiz. Noveishie Tekhnol.*, **28**, No. 9: 1143 (2006).
67. T.M. Radchenko, O.S. Gatsenko, V.V. Lizunov, and V.A. Tatarenko, Research trends and statistical-thermodynamic modeling the α '-Fe₁₆N₂-based phase for permanent magnets, *Fundamentals of Low-Dimensional Magnets, 1st Edition* (Eds. R.K. Gupta, S.R. Mishra, and T.A. Nguyen) (Taylor & Francis–CRC Press: 2022), Ch. 18, p. 343;
<https://doi.org/10.1201/9781003197492-18>
68. V.V. Slezov, *Theory of Diffusive Decomposition of Solid Solutions* (Chichester: Harwood Academic: 1995).

Received 04.11.2024
Final version 11.11.2024

В.А. Татаренко, Т.М. Радченко, А.Ю. Научук, Б.М. Мордюк
Інститут металофізики ім. Г.В. Курдюмова НАН України,
бульв. Академіка Вернадського, 36,
03142 Київ, Україна

ПАРАМЕТЕРИЗАЦІЯ ДИФУЗІЙНИХ ХАРАКТЕРИСТИК КІНЕТИКИ РЕЛАКСАЦІЇ АТОМНОГО ПОРЯДКУ У СПЛАВАХ Ni–Al

Для дослідження дифузійних характеристик сплавів заміщення ГЦК-Ni–Al розглянуто, проаналізовано та застосовано кінетичні моделі, в яких релаксація параметрів кореляції у взаємному розташуванні атомів зумовлює часову залежність як інтенсивності дифузного розсіяння випромінювання I , так і залишкового електроопору ρ . За допомогою параметеризації наявних літературних даних стосовно вимірювання залишкового електроопору впродовж ізотермічного відпалу сплавів оцінено найбільш характерні часи релаксації ρ після загартування сплавів, а також рівноважні значення ρ_{∞} . Визначено максимальний характерний час релаксації атомного порядку таких сплавів, а за гіпотезою про збіг найбільших характерних часів релаксації для I та ρ передбачено криві часової залежності нормованої зміни інтенсивності ΔI . Релаксаційний процес супроводжується збільшенням як кількості кластерів з наявністю близького порядку в їхній структурі, так і ступеня їхньої впорядкованості, що узгоджується з результатами комп'ютерного моделювання локального атомного порядку за методом Монте-Карло та із моделлю неоднорідного близького порядку.

Ключові слова: твердий розчин Ni–Al, атомні стрибки, дифузія, близький порядок, релаксація, дифузне розсіяння, залишковий електроопір.